

# Infrared Spectra of Protonated Neurotransmitters: Serotonin

Anita Lagutschenkov,<sup>†</sup> Judith Langer,<sup>†</sup> Giel Berden,<sup>‡</sup> Jos Oomens,<sup>‡,§</sup> and Otto Dopfer<sup>\*,†</sup>

*Institut für Optik und Atomare Physik, Technische Universität Berlin, Hardenbergstrasse 36, 10623 Berlin, Germany, FOM Institute for Plasma Physics Rijnhuizen, Edisonbaan 14, 3439 MN Nieuwegein, The Netherlands, and University of Amsterdam, Science Park 904, Amsterdam 1098XH, The Netherlands*

Received: September 29, 2010; Revised Manuscript Received: November 4, 2010

The gas-phase IR spectrum of the protonated neurotransmitter serotonin (5-hydroxytryptamine) was measured in the fingerprint range by means of IR multiple photon dissociation (IRMPD) spectroscopy. The IRMPD spectrum was recorded in a Fourier transform ion cyclotron resonance mass spectrometer coupled to an electrospray ionization source and an IR free electron laser. Quantum chemical calculations at the B3LYP and MP2 levels of theory using the cc-pVDZ basis set yield six low-energy isomers in the energy range up to 40 kJ/mol, all of which are protonated at the amino group. Protonation at the indole N atom or the hydroxyl group is substantially less favorable. The IRMPD spectrum is rich in structure and exhibits 22 distinguishable features in the spectral range investigated (530–1885 cm<sup>-1</sup>). The best agreement between the measured IRMPD spectrum and the calculated linear IR absorption spectra is observed for the conformer lowest in energy at both levels of theory, denoted **g-1**. In this structure, one of the three protons of the ammonium group points toward the indole subunit, thereby maximizing the intramolecular NH<sup>+</sup>– $\pi$  interaction between the positive charge of the ammonium ion and the aromatic indole ring. This mainly electrostatic cation– $\pi$  interaction is further stabilized by significant dispersion forces, as suggested by the substantial differences between the DFT and MP2 energies. The IRMPD bands are assigned to individual normal modes of the **g-1** conformer, with frequency deviations of less than 29 cm<sup>-1</sup> (average <13 cm<sup>-1</sup>). The effects of protonation on the geometric and electronic structure are revealed by comparison with the corresponding structural, energetic, electronic, and spectroscopic properties of neutral serotonin.

## 1. Introduction

5-hydroxytryptamine (5-HT), also known as serotonin (Figures 1 and 2), is a representative of the group of biogenic monoamine neurotransmitters. Neurotransmitters are endogenous chemical messenger compounds, which are responsible for signal transmission, enhancement, and modulation in the central and sympathetic nervous systems. Serotonin is biochemically derived from L-tryptophan and is found in the non-neuronal tissues of the gastrointestinal tract, in blood platelets, in the cardiovascular system, and in the nervous system of humans and animals. Serotonin possesses a complex pharmacology, and at least seven different serotonin-receptor families (denoted 5-HT<sub>n</sub> with *n* = 1–7) with various subtypes are known. The diversity of the many different serotonin receptors leads to control and regulation of a large variety of physiological and behavioral processes.<sup>1</sup> Thus, serotonin plays an important role in the regulation of body temperature, blood pressure, regulation of smooth muscle functions in cardiovascular and gastrointestinal tissue, sleep, mood, appetite, aggression, anger, and sexuality. Low serotonin levels or improper serotonin receptor functionalities are considered to lead to aggressive behavior, depression, obsessive-compulsive disorders,<sup>2</sup> migraine, bipolar disorder, anxiety, and borderline personality disorder.<sup>3</sup> Abnormalities in several serotonergic brainstems are suspected to play a role in sudden infant death syndrome.<sup>4</sup>

The conformational flexibility of ethylamine neurotransmitters, mainly arising from facile rotations around the C–N and two C–C bonds of the ethylamine side chain, is expected to be highly relevant for the drug–receptor interaction and molecular recognition.<sup>5</sup> At physiological pH values, serotonin occurs in its protonated form,<sup>5–7</sup> denoted serotoninH<sup>+</sup>, with strong preference for protonation at the terminal amino group of the alkylamine side chain (Figure 2). The high-affinity binding site of the various 5-HT receptors is expected to involve a strong interaction between the positively charged amino group of serotoninH<sup>+</sup> and the matching recognition site, often via intermolecular cation– $\pi$  interactions.<sup>5,7–9</sup> Binding of serotoninH<sup>+</sup> to the receptor induces a conformational change, which in turn triggers the signal transduction. Thus, in order to understand these processes at the molecular level and to support drug design of targeting serotonergic systems, it is of fundamental interest to evaluate the possible conformations of isolated serotonin and its protonated form, as well as their interaction with an environment (e.g., solvation).<sup>5</sup>

Neutral<sup>10–12</sup> and protonated<sup>5,8,13–15</sup> serotonin has been investigated theoretically with respect to its conformations in the gas phase and in aqueous solution. Calculations for isolated serotonin yield a large number of isomers within a narrow energy range. For example, Van Mourik and Emson found 23 low-energy isomers for serotonin within 11 kJ/mol at the B3LYP/6-31+G\* level.<sup>10</sup> These results were confirmed by Le Greeve et al., who also report energies obtained at the MP2 level.<sup>12</sup> Protonation significantly reduces the number of low-lying isomers. Most studies consider six low-energy isomers (plus their equivalent mirror images).<sup>5,8,13–15</sup> Alagona and Ghio provide a detailed structural, energetic, and IR spectroscopic

\* Corresponding author. E-mail: dopfer@physik.tu-berlin.de. Fax: (+49) 30-31423018.

<sup>†</sup> Technische Universität Berlin.

<sup>‡</sup> FOM Institute for Plasma Physics Rijnhuizen.

<sup>§</sup> University of Amsterdam.

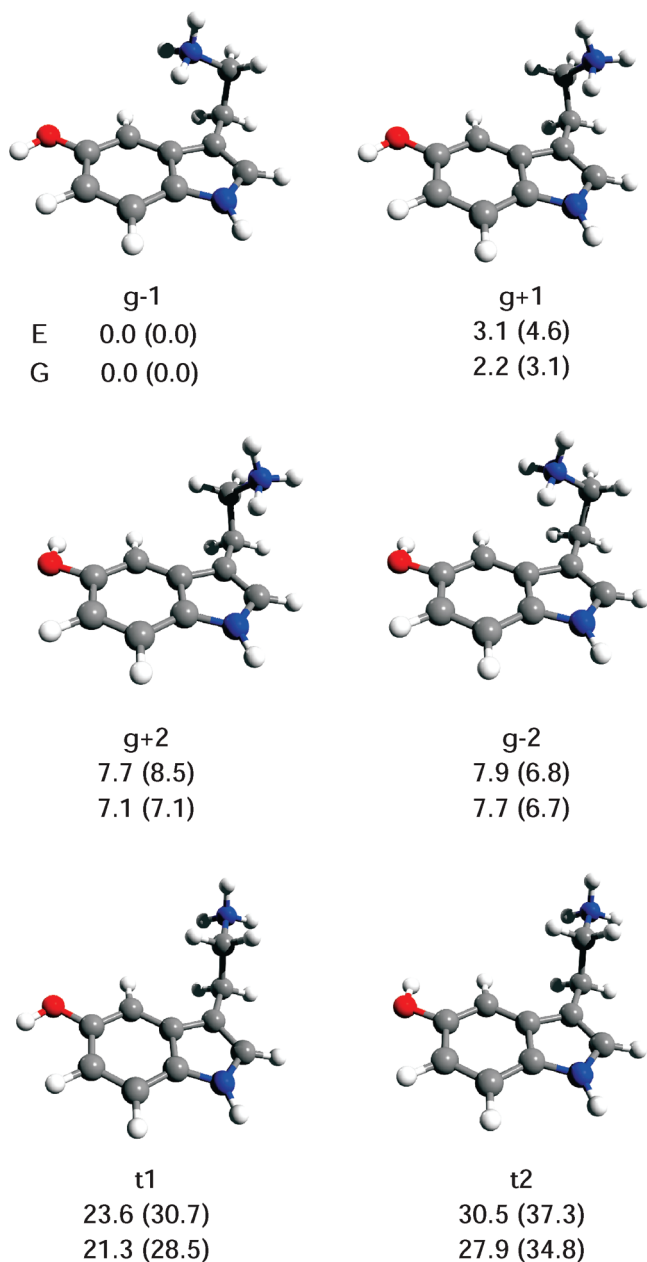


**Figure 1.** Structures and relative energies ( $\Delta E$ , top) and free energies ( $\Delta G$ , bottom) of the six most stable isomers of serotoninH<sup>+</sup> derived at the B3LYP/cc-pVDZ level. Relative energies obtained at the MP2/cc-pVDZ level are given in parentheses. All values in kJ/mol.

analysis of three main isomers of serotoninH<sup>+</sup> (two gauche and one trans isomer), all with the extra proton located at the amino group (for the definition of gauche and trans, see Figures 1 and 2 and *vide infra*).<sup>15</sup> The gauche isomers are clearly favored with respect to the trans isomer by up to 30 kJ/mol at all theoretical levels considered due to intramolecular cation- $\pi$  interactions. However, when solvation effects are taken into account, the trans isomer experiences stronger stabilization by the solvent than the gauche isomers, leading to comparable energies of both the gauche and trans isomers in solution. In a further quantum chemical study, Manivet and co-workers find the same low energy isomers for isolated serotoninH<sup>+</sup> (in total, six within 31.5 kJ/mol at the B3LYP/6-31+G(d,p) level), again with a clear preference for gauche over trans conformers due to the intramolecular cation- $\pi$  interactions of the positively charged ammonium group with the aromatic  $\pi$  electron system.<sup>14</sup>

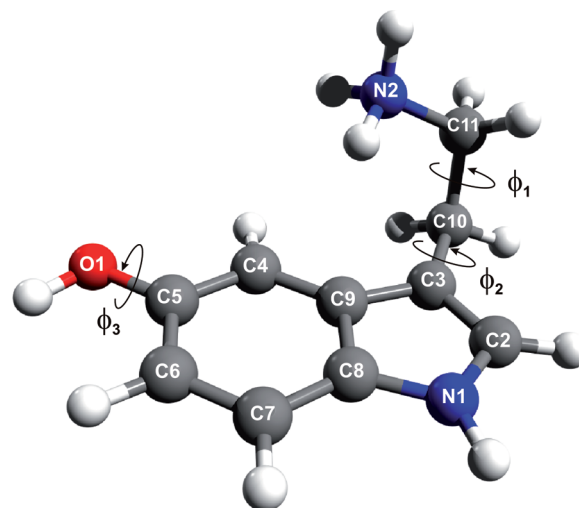


**Figure 2.** Definition of torsional angles defining the conformation of the various possible isomers of serotoninH<sup>+</sup>. Positions/angles of  $\phi_1$  and  $\phi_2$  are responsible for the differentiation between gauche (here also + or -) and trans isomers.  $\phi_3$  describes the relative orientation of the hydroxyl group and the indole nitrogen atom, leading to a further index describing the conformers with 1 (syn) or 2 (anti).

So far, spectroscopic gas-phase approaches have been limited to neutral serotonin. The conformational preferences of the isolated molecule have been elucidated in supersonic jets by LeGreve et al.,<sup>12,16</sup> using a variety of spectroscopic techniques, including resonant two-photon ionization, laser-induced fluorescence, and UV-UV and IR-UV hole-burning techniques. They identified a set of eight isomers present in the cold molecular beam expansion. Bayari et al. presented Fourier transform infrared (FT-IR) spectra of serotonin in KBr films as well as in aqueous solution.<sup>11</sup> However, these spectra display low resolution, and it is unclear at present whether they correspond to the neutral or the protonated form. Experiments on serotoninH<sup>+</sup> were mainly limited to the condensed phase,<sup>5-7,17,18</sup> due to the inherent problem of the low number densities of charged species in the gas phase. All of these experiments show that serotoninH<sup>+</sup> occurs in trans configuration in crystal structures<sup>18,19</sup> and also in solution,<sup>7,17</sup> due to effective stabilization of the ammonium group by counterions and solvent molecules. For example, Beene et al. describe the in situ identification of intermolecular cation- $\pi$  binding between serotonin and Trp183 of the serotonin channel 5-HT<sub>3A</sub>R.<sup>7</sup> Experimental information on the structure of isolated serotoninH<sup>+</sup> is restricted to mass spectrometric data,<sup>20,21</sup> which mainly provide fragmentation pathways observed after collisional activation and thus only very indirect information about the geometry. Although the facile elimination of NH<sub>3</sub> upon collision-induced dissociation is consistent with the predicted preferential protonation at the terminal amino group of the ethyl side chain, no unambiguous spectroscopic confirmation of the protonation site is available. Thus, the present IR spectroscopic study of isolated serotoninH<sup>+</sup> provides the first experimental information about the conformation and protonation site of this fundamental biogenic amine neurotransmitter in the gas phase.

Only a few protonated neurotransmitters have been investigated spectroscopically so far. Recent pioneering IR spectroscopic studies on protonated neurotransmitters and analogues by Simons and co-workers include ethanolamineH<sup>+</sup>, ephedrineH<sup>+</sup>, pseudoephedrineH<sup>+</sup>, 1-phenylethylamineH<sup>+</sup>, and 2-amino-1-phenylethanolH<sup>+</sup>.<sup>22</sup> In these experiments, protonation is accomplished by ionization-induced intracuster proton transfer

occurring in a hydrogen-bonded phenol-neurotransmitter cluster. This approach produces a phenoxy-neurotransmitterH<sup>+</sup> dimer, the structure of which is subsequently probed by IR photodissociation spectroscopy monitoring the loss of the phenoxy radical. Alternatively, the neurotransmitterH<sup>+</sup> can directly be produced upon postionization fragmentation and then probed by IR multiple photon dissociation (IRMPD). Owing to this complex photochemical production mechanism, the observed protonation site may not necessarily correspond to the energetically most favorable one of the isolated neurotransmitterH<sup>+</sup>, in particular because barriers for proton migration can be substantial in bio-organic molecules. Moreover, this approach is limited to neurotransmitters and other biomolecules, which can be transferred into the gas phase by thermal heating. As an alternative, electrospray ionization (ESI) offers a more general route to efficiently generate isolated protonated biomolecules in the gas phase. In particular, IR photodissociation spectroscopy coupled with ESI sources and tandem mass spectrometry, in fruitful combination with quantum chemical calculations, has proven to be an efficient tool to characterize the structure of isolated protonated (bio)organic molecules in the gas phase, with a particular focus on the determination of the preferred site of protonation.<sup>23,24</sup> Alternative techniques to unravel the protonation sites and conformations of protonated biomolecules and their clusters include IR hole-burning spectroscopy of ESI-prepared ions in cryogenic ion traps.<sup>25</sup> For bare protonated ions, often IRMPD is required to overcome the high dissociation thresholds of these strongly bound ions. IRMPD spectroscopy is commonly realized through the successful coupling of tandem mass spectrometers and ion traps with intense IR free electron lasers (IR-FELs) providing tunable IR radiation in the informative fingerprint spectral range (50–2500 cm<sup>-1</sup>). The structures of a plethora of (bio)organic and metal–organic ions and their complexes have been characterized recently by IRMPD using this strategy.<sup>23,24,26</sup>

In a recent campaign, IRMPD spectra of a series of ESI-generated protonated neurotransmitters (dopamine, histamine, serotonin) were recorded in the fingerprint range in a Fourier transform ion cyclotron resonance mass spectrometer (FT-ICR-MS), which was coupled to the IR beamline of the Free Electron Laser for Infrared eXperiments (FELIX).<sup>27</sup> A detailed account of the results for dopamineH<sup>+</sup> has been given elsewhere.<sup>28</sup> The present work provides a detailed analysis of the IRMPD spectrum of serotoninH<sup>+</sup> utilizing quantum chemical calculations at the B3LYP and MP2 levels of theory.

## 2. Experimental and Theoretical Techniques

The IRMPD spectrum of serotoninH<sup>+</sup> was recorded in the fingerprint range (530–1885 cm<sup>-1</sup>) in a FT-ICR-MS equipped with an ESI source and coupled to the IR beamline of FELIX.<sup>24,29</sup> Serotonin was purchased from Sigma-Aldrich as solid serotonin hydrochloride in analytical reagent grade and used without further purification. SerotoninH<sup>+</sup> ions were produced by spraying a  $\sim 1 \times 10^{-5}$  molar solution of serotonin hydrochloride dissolved in water/methanol (1:4) at a flow rate of  $\sim 10 \mu\text{L min}^{-1}$ . After accumulation in a hexapole ion trap for 4 s, the ESI-generated ions were transferred into the ICR trap via an octopole ion guide. Subsequently, serotoninH<sup>+</sup> ions were mass selected in the ion trap and irradiated for 2 s with 10 macropulses from FELIX operating at a repetition rate of 5 Hz. The average macropulse energy was measured to be around 40 mJ. The bandwidth of the FELIX radiation is  $\sim 0.5\%$  of the central wavelength (full width at half-maximum (fwhm)), which corresponds to 5 cm<sup>-1</sup> at 1000 cm<sup>-1</sup>. Calibration of the laser

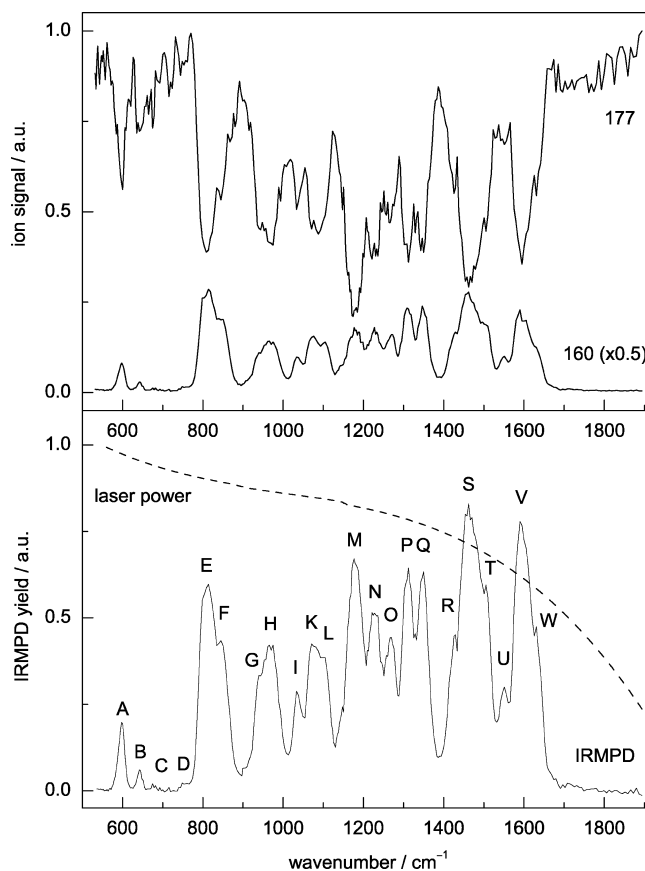


**Figure 3.** Upper panel: Ion currents of the protonated serotonin parent ion ( $m = 177$  u) and the fragment channel ( $m = 160$  u). Lower panel: IRMPD spectrum of protonated serotonin recorded in the fingerprint range (530–1885 cm<sup>-1</sup>). The IRMPD yield is normalized linearly for IR laser power (dashed line).

wavelength was achieved using a grating spectrometer with an accuracy of  $\pm 0.02 \mu\text{m}$ , which corresponds to  $\pm 0.5$  and  $\pm 8$  cm<sup>-1</sup> at frequencies of 500 and 2000 cm<sup>-1</sup>, respectively. Depending on the laser frequency, the step size varied between 2 and 7 cm<sup>-1</sup>. The single fragmentation channel observed upon IRMPD of serotoninH<sup>+</sup> ( $m = 177$  u) was  $m = 160$  u. Parent and fragment ion intensities were monitored as a function of the laser frequency, and the IRMPD yield was then calculated as the integrated intensity of the fragment ions divided by the sum of parent and fragment ion intensities. The IRMPD yield was linearly normalized for variations in the laser intensity.

Quantum chemical calculations at the B3LYP and MP2 levels of theory using the cc-pVDZ basis set<sup>30</sup> were performed for serotonin and serotoninH<sup>+</sup> in order to identify various low-lying isomers on the potential energy surface and to evaluate their structure, energetics, and IR spectral properties.<sup>31</sup> Harmonic vibrational frequencies were scaled by 0.98 (B3LYP) and 0.97 (MP2).<sup>28</sup> All reported energies are corrected for scaled zero point energies. For all minima, harmonic frequency analysis ensured their nature as local or global minima on the potential energy surface. Theoretical IR stick spectra are convoluted with a width (fwhm) of 30 cm<sup>-1</sup> to facilitate convenient comparison with the experimental spectrum. A natural bond order (NBO) analysis was performed in order to derive atomic charge distributions of the isomers of interest.

## 3. Results and Discussion

The IRMPD spectrum of serotoninH<sup>+</sup> reproduced in Figure 3 is highly structured and reveals 22 major transitions in the

**TABLE 1: Experimental Vibrational Frequencies of SerotoninH<sup>+</sup> (IRMPD Spectrum, Figure 5) Compared to Frequencies of the g-1 Isomer Calculated at the B3LYP/cc-pVDZ Level of Theory**

serotoninH <sup>+</sup> <sup>a</sup> $\nu_{\text{exp}}/\text{cm}^{-1}$	g-1 <sup>b,c</sup> $\nu_{\text{calc}}/\text{cm}^{-1}$	vibration <sup>d</sup>
1624 (-) W	1650 (29)	arom. $\sigma_{\text{CC}}$ ( $\nu_{8a}$ )
1583 (58) V	1595 (84)	arom. $\sigma_{\text{CC}}$ ( $\nu_{8b}$ )
	1592 (87)	$\beta_{\text{NH}_3}$ asym.
	1582 (37)	$\beta_{\text{NH}_3}$ asym.
1542 (47) U	1552 (10)	arom. $\sigma_{\text{CC}}$
1499 (-) T	1508 (19)	arom. $\sigma_{\text{CC}}$ ( $\nu_{19b}$ )
1454 (60) S	1465 (68)	arom. $\sigma_{\text{CC}}$ ( $\nu_{19a}$ )
	1445 (51)	$\beta_{\text{NH}_3}$ sym. coupled to CH <sub>2</sub> (scissor, C11) out-of-phase
	1439 (48)	$\beta_{\text{NH}_3}$ sym. coupled to CH <sub>2</sub> (scissor, C11) in-phase
1417 (-) R	1426 (9)	$\sigma_{\text{CC}}$ coupled to $\sigma_{\text{CN}}$
	1419 (13)	$\beta_{\text{CH}_2}$ (scissor, C10)
1342 (39) Q	1371 (85)	arom. $\sigma_{\text{CC}}$ ( $\nu_{14}$ )
	1365 (8)	$\beta_{\text{CH}_2}$ (wagging, C11)
	1345 (30)	$\beta_{\text{CH}_2}$ (wagging, C10)
	1331 (18)	arom. $\beta_{\text{CH}}$
1304 (40) P	1316 (57)	$\sigma_{\text{CO}}$
	1288 (14)	$\tau_{\text{CH}_2}$ (torsion, C11)
1263 (41) O	1253 (44)	arom. $\beta_{\text{CH}}$
	1240 (6)	arom. $\beta_{\text{CH}}$
1220 (42) N	1213 (30)	$\tau_{\text{CH}_2}$ (torsion, C10)
	1209 (5)	arom. $\beta_{\text{CH}}$
1170 (49) M	1166 (120)	$\delta_{\text{OH}}$
	1129 (8)	arom. $\beta_{\text{CH}}$ (C6/C7)
1094 (29) L	1098 (19)	arom. $\beta_{\text{NH/CH}}$ (N1/C2)
1066 (54) K	1074 (13)	CH <sub>2</sub> twist (CH <sub>2</sub> /CH <sub>2</sub> /NH <sub>3</sub> ) C10
	1060 (19)	CH <sub>2</sub> twist (CH <sub>2</sub> /CH <sub>2</sub> /NH <sub>3</sub> ) C11
1027 (37) I	1016 (14)	aliph. $\sigma_{\text{CC}}$ (C3-C10)
961 (38) H	964 (4)	aliph. $\sigma_{\text{CCN}}$ (C10-C11-N2, asym.)
936 (28) G	936 (27)	ring
	928 (0)	arom. $\gamma_{\text{CH}}$ (C6/C7)
	894 (5)	CH <sub>2</sub> twist (CH <sub>2</sub> /CH <sub>2</sub> /NH <sub>3</sub> ) NH <sub>3</sub>
840 (30) F	845 (28)	aliph. $\sigma_{\text{CCN}}$ (C10-C11-N2, sym.)
808 (40) E	821 (3)	arom. $\gamma_{\text{CH}}$ (out-of-phase C2/C4)
	817 (16)	arom. $\gamma_{\text{CH}}$ (in-phase C2/C4)
	810 (35)	arom. $\gamma_{\text{CH}}$
	804 (8)	arom. $\gamma_{\text{CH}}$
	797 (24)	arom. $\gamma_{\text{CH}}$
751 (34) D	754 (3)	arom. $\gamma_{\text{CC}}$ ( $\nu_4$ )
	748 (0)	ring ( $\nu_{6a}$ )
678 (22) C	671 (5)	ring
640 (17) B	648 (4)	arom. $\gamma_{\text{CC}}$
595 (20) A	608 (16)	arom. $\gamma_{\text{CC}}$
	573 (4)	ring

<sup>a</sup> Peak positions taken from the IRMPD spectrum; the fwhm is given in parentheses (see Figure 5 for labels of the transitions). <sup>b</sup> IR intensities in km/mol are given in parentheses. <sup>c</sup> Harmonic frequencies are scaled by 0.98. <sup>d</sup> The notation  $\sigma$ ,  $\gamma$ ,  $\beta$ , and  $\tau$  refers to stretch, out-of-plane bend, in-plane bend, and torsional modes, respectively. The notation  $\nu_x$  is adopted from the Wilson notation for substituted benzene molecules.<sup>33</sup>

spectral range between 530 and 1885 cm<sup>-1</sup>, labeled A–W (Table 1). The IRMPD spectrum was extracted from the fragment channel with  $m = 160$  u. No other significant fragment channel was observed. The depletion spectrum of the parent ion ( $m = 177$  u) is also shown for comparison in Figure 3, along with the appearance spectrum observed in the daughter ion channel. The depletion signal exceeds 50% for many resonances, indicating efficient IRMPD under the present experimental conditions. As the IRMPD yield is normalized for variations of the parent ion production in the ESI source, the IRMPD spectrum displays better signal-to-noise ratio than the depletion signal of the parent ion. Thus, the IRMPD yield is used for comparison with the IR spectra calculated for the various serotoninH<sup>+</sup> isomers. The minimal width of transitions observed in the IRMPD spectrum is about 20 cm<sup>-1</sup> and attributed to several factors, including the finite laser bandwidth of 0.5% ( $\Delta\nu = 2.5\text{--}10$  cm<sup>-1</sup> for  $\nu = 500\text{--}2000$  cm<sup>-1</sup>), spectral congestion due to overlapping vibrational transitions and possible contribu-

tions from several isomers, unresolved rotational substructure ( $T = 300$  K for ions in the ICR cell), and spectral broadening arising from the multiple photon absorption process.<sup>32</sup>

Quantum chemical calculations were performed to establish the vibrational and isomer assignment of the transitions observed in the IRMPD spectrum. Previous calculations reported six low-lying isomers of serotoninH<sup>+</sup> with protonation at the N atom of the terminal amino group.<sup>8,14</sup> These isomers were also identified in the current study (Figure 1). Further isomers with the excess proton attached to the N atom of the indole ring or to the O atom of the hydroxyl group were also considered (Figure F1 in the Supporting Information). As these protonation sites are much higher in energy (100–170 kJ/mol), these isomers are not discussed in detail here. Conformers which are mirror images of the structures shown in Figure 1 are also omitted, as they are symmetry-equivalent and have the same properties. The nomenclature to distinguish the individual serotoninH<sup>+</sup> conformers in Figure 1 is adapted from that used previously for

dopamineH<sup>+</sup>.<sup>28</sup> This nomenclature describes the relative orientation of the ethylamine side chain and the hydroxyl group to the aromatic indole ring for the N-protonated serotoninH<sup>+</sup> isomers. The atom numbering and relevant angular coordinates are indicated in Figure 2. The notation **g** and **t** describes isomers, in which the ammonium group of the ethylamine unit is oriented gauche or trans with respect to the indole moiety. In the **g** isomers the ammonium group is pointing toward the indole ring ( $-90^\circ < \phi_1 < +90^\circ$ ), while in the **t** isomers it points away from it ( $\phi_1 > 90^\circ$  or  $< -90^\circ$ ). The gauche isomers are further divided into those with positive and negative  $\phi_1$  values, as indicated by **g**<sup>+</sup> and **g**<sup>-</sup>, respectively. All gauche and trans isomers can further be classified by the orientation of the hydroxyl group described by  $\phi_3$ . The notation **1** and **2** differentiates isomers, in which the hydroxyl group is either in syn (**1**) or in anti (**2**) orientation with respect to the indole N atom.

In general, there is good agreement between the relative energies ( $\Delta E$ ) and free energies ( $\Delta G$ ) of the serotoninH<sup>+</sup> isomers calculated at the B3LYP and MP2 levels of theory (Figure 1). For example, for the four lowest-energy structures lying below 10 kJ/mol (all **g** isomers), the agreement is better than  $\pm 1.5$  kJ/mol. Both theoretical levels predict the **g-1** isomer to be the global minimum on the potential energy surface. In this isomer, the ammonium group interacts preferentially with the phenol ring via NH<sup>+</sup> $-\pi$  interaction. The **g+1** isomer is slightly less stable than **g-1**, with an energy gap of 3.1 (4.6) kJ/mol at the B3LYP (MP2) level. In this isomer, the ammonium group interacts with the pyrrole ring via NH<sup>+</sup> $-\pi$  interaction. The two isomers are separated by a substantial barrier of 4.8 kJ/mol (B3LYP) for **g+1**  $\rightarrow$  **g-1** (i.e., 7.9 kJ/mol for **g+1**  $\leftarrow$  **g-1**), indicating that the internal rotation of the ammonium group above the indole plane is strongly hindered. Similar barrier heights have been reported previously, e.g. 5.3 kJ/mol for **g+1**  $\rightarrow$  **g-1** at the B3LYP/6-31+G(d,p) level.<sup>14</sup> As a general trend, the **g $\pm$ 2** structures are less stable than the **g $\pm$ 1** isomers by 5–10 kJ/mol. Apparently, the ion–dipole interaction between the positively charged ammonium group and the polar OH bond favors an orientation in which the hydroxyl group points away from the NH<sub>3</sub><sup>+</sup> unit. Interestingly, the energetic order predicted by B3LYP and MP2 differs for the **g+2** and **g-2** structures, which are, however, close in energy. B3LYP prefers **g+2** slightly over **g-2** by 0.2 kJ/mol, whereas MP2 yields an energetic preference for **g-2** over **g+2** by 1.7 kJ/mol. The two **t** isomers, **t1** and **t2**, are considerably less stable than the corresponding **g** isomers by  $\sim 20$ – $30$  kJ/mol, because they lack the cation– $\pi$  interaction of the ammonium group with the indole ring. The barrier between the **t1** isomer and **g-1** is appreciable and amounts to 10.1 kJ/mol for **t1**  $\rightarrow$  **g-1** at the B3LYP level (i.e., 33.7 kJ/mol for **t1**  $\leftarrow$  **g-1**). A similar barrier of 9.0 kJ/mol was previously obtained at the B3LYP/6-31+G(d,p) level.<sup>14</sup> Although there is in general good agreement between the relative energies of the various isomers calculated at the MP2 and B3LYP levels, there is a systematically larger energy difference between corresponding **g** and **t** isomers at the MP2 level. The relative energies of the **t** isomers are higher by 7 kJ/mol at the MP2 level than at the B3LYP level. This additional relative stabilization of the **g** isomers with respect to the **t** isomers at the MP2 level is attributed to dispersion interactions of the ammonium group with the aromatic indole ring, which are relevant only for the **g** isomers and are neglected in the B3LYP calculations.<sup>15</sup> These additional dispersion forces of the intramolecular NH– $\pi$  bond also lead to a shorter distance between the proton donor of the ammonium group and the aromatic ring at the MP2 level (by  $\sim 0.09$  Å for **g-1**). Similar effects have

**TABLE 2: Selected Bond Distances (in Å), Dihedral Angles (in Degrees), and Relative Energies and Free Energies (in kJ/mol) of the Protonated Serotonin Isomers **g-1** and **t1** Calculated at the B3LYP and MP2 Levels (Figures 1 and 2)<sup>a</sup>**

	<b>g-1</b>		<b>t1</b>	
	B3LYP	MP2	B3LYP	MP2
$\phi_1$	-54.7	-52.8	-173.5	-173.3
$\phi_2$	-94.2	-91.6	-107.4	-107.6
$\phi_3$	175.4	173.8	178.3	177.3
$R_{\text{NH}\cdots\text{C3}}$	2.430	2.322		
$R_{\text{NH}\cdots\text{C4}}$	2.468	2.485		
$R_{\text{NH}\cdots\text{C9}}$	2.312	2.220		
$\Delta E$	0.0	0.0	23.6	30.7
$\Delta G$	0.0	0.0	21.3	28.5

<sup>a</sup>  $\phi_1$  = dihedral angle C3C10C11N2,  $\phi_2$  = dihedral angle C2C3C10C11,  $\phi_3$  = dihedral angle C4C5O1H.

previously been noted for dopamineH<sup>+</sup>,<sup>28</sup> and to a lesser extent for neutral serotonin,<sup>12</sup> demonstrating the substantial contribution of dispersion for these intramolecular cation– $\pi$  interactions. Density functional calculations using functionals neglecting (B3LYP, B2LYP) and including dispersion (B3LYP-D, B2LYP-D, M06-2X) confirm that the additional stabilization of 7 kJ/mol for the **g** isomers predicted at the MP2 level is indeed due to dispersion and not due to intramolecular basis set superposition error or possible overestimation of dispersion energy at the MP2 level (Table T1 in the Supporting Information). Further serotoninH<sup>+</sup> structures with the excess proton attached to the N atom of the indole ring or at the O atom of the hydroxyl group are less stable by  $\sim 100$  and  $\sim 170$  kJ/mol than the **g-1** isomer, respectively, at both levels of theory (Figure F1 in the Supporting Information). Protonation of primary amines at the amino group is clearly favored in the gas phase.

Table 2 summarizes selected structural and energetic parameters for the most stable gauche and trans isomers of serotoninH<sup>+</sup>, **g-1** and **t1**. The dihedral angles ( $\phi_1$ – $\phi_3$ ) describing the conformation of the alkyl side chain and the orientation of the hydroxyl group are listed along with selected bond lengths and relative energies. The corresponding data for all other calculated isomers are provided in Table T2 in the Supporting Information. All bond lengths of **g-1** are given in Figure F2 in the Supporting Information. As mentioned above, the **g-1** global minimum is significantly stabilized by the NH<sup>+</sup> $-\pi$  cation– $\pi$  interaction between the positively charged ammonium group and the aromatic indole ring, which involves a short intramolecular NH–C9 bond length of 2.312 (2.220) Å at the B3LYP (MP2) level. As a consequence of the substantial NH<sup>+</sup> $-\pi$  interaction, the N–H bond of the proton donor of the ammonium group is substantially elongated (1.042 Å, B3LYP) as compared to the corresponding free N–H bond lengths (1.028 Å). The most stable isomer of neutral serotonin, denoted **g+2(n)** and shown in Figure F2 in the Supporting Information, has a structure in which one of the H atoms of the nearly neutral amino group interacts with the C2 atom of the pyrrole ring. It exhibits a much weaker NH– $\pi$  interaction as compared to the **g-1** isomer of serotoninH<sup>+</sup>, as evidenced by the relatively long NH–C3 bond lengths of 2.767 (2.629) Å.

The IRMPD spectrum of serotoninH<sup>+</sup> is compared in Figure 4 to the calculated linear IR absorption spectra of all considered isomers obtained at the B3LYP level. The spectra calculated at the MP2 level are similar in appearance and thus not discussed further here. This comparison reveals a single isomer to be mainly responsible for the observed IRMPD spectrum (Figure

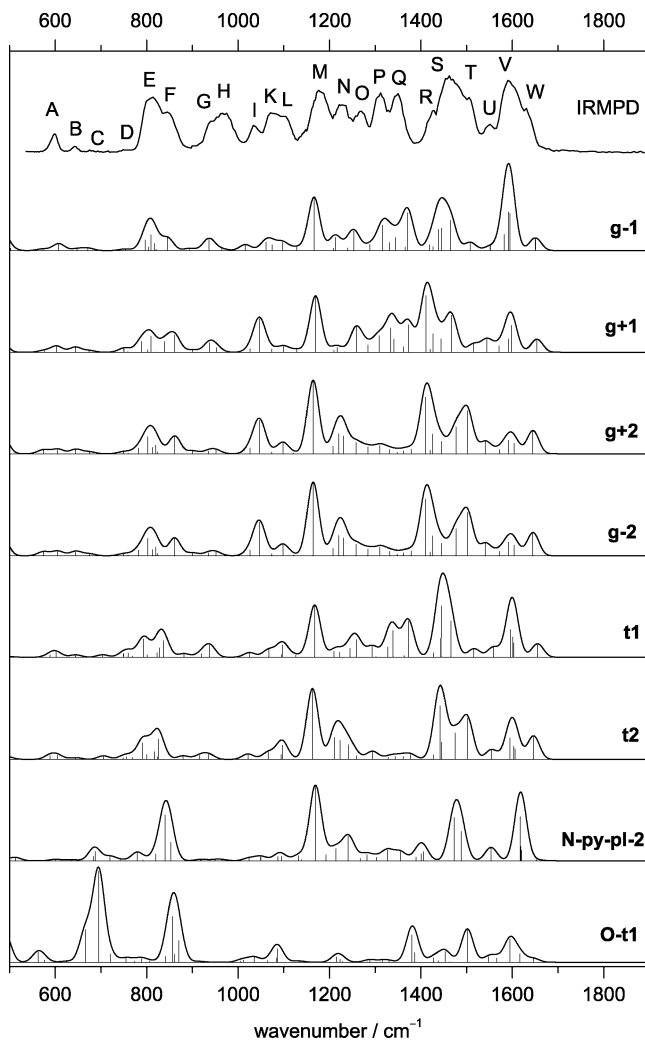


**Figure 4.** IRMPD spectrum of serotoninH<sup>+</sup> and B3LYP/cc-pVDZ spectra of calculated isomers of serotoninH<sup>+</sup> in energetic order (scaled by 0.98 with a fwhm of 30 cm<sup>-1</sup>). The calculated intensities are all on the same scale.

4), namely the most stable **g-1** structure. Both the band positions and relative intensities of this isomer provide the closest match to the experimental spectrum. The other gauche isomers, namely **g+1**, **g+2**, and **g-2**, although close in energy and therefore potentially present in the ion cloud at room temperature, have a very intense transition predicted near 1400 cm<sup>-1</sup>, which is nearly absent in the IRMPD spectrum. This mode arises from a bending mode of the ammonium group ( $\beta_{\text{NH}_3}$ ) slightly coupled to CH<sub>2</sub> bending modes. Similarly, these three gauche isomers feature a relatively intense transition near 1050 cm<sup>-1</sup>, which is also not prominent in the IRMPD spectrum. Thus, significant contributions from gauche isomers other than **g-1** can be excluded as major carriers of the IRMPD spectrum. This scenario is consistent with thermodynamic considerations. Assuming thermodynamic equilibrium at 300 K, the relative energies  $\Delta E$  ( $\Delta G$ ) calculated at the B3LYP level suggest a population ratio of 1:0.29:0.045:0.042 (1:0.41:0.058:0.045) for **g-1**, **g+1**, **g+2**, and **g-2**, which also yields a clear preference for the **g-1** isomer (>65%). As the **t2** isomer exhibits very weak activity in the 1300–1350 cm<sup>-1</sup> range, in which strong resonances are detected in the IRMPD spectrum (bands P and Q), this structure can also be excluded as major carrier. The **t1** isomer has in fact a spectrum similar to that of the **g-1** isomer in the fingerprint range and can thus not be excluded by spectroscopic arguments. Nonetheless, on the basis of its high

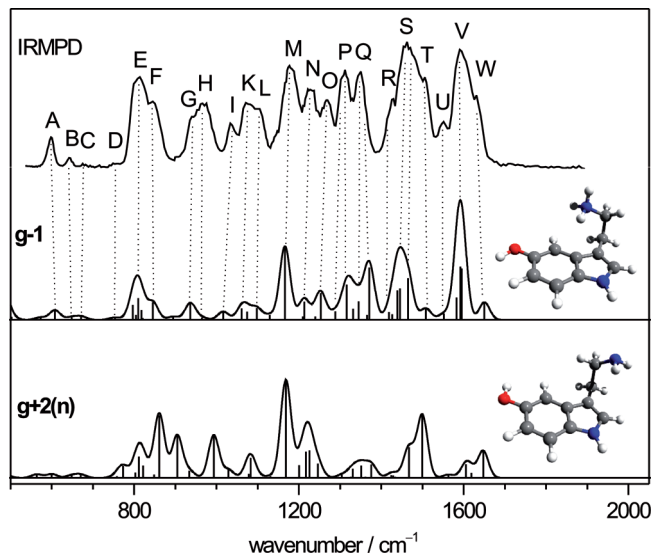


**Figure 5.** Comparison of the IRMPD spectrum of serotoninH<sup>+</sup> with the linear IR absorption spectra for the most stable gauche isomers of serotoninH<sup>+</sup>, **g-1**, and neutral serotonin, **g+2(n)**, calculated at the B3LYP/cc-pVDZ level. Corresponding transitions are connected by dotted lines.

energy (20–30 kJ/mol above **g-1**) and the at most minor contributions of the lower-lying **g+1**, **g+2**, and **g-2** isomers, it may be excluded for thermodynamic reasons. Comparison of the IRMPD spectrum with the calculated spectra may indeed suggest minor contributions from **t2**, **g+1**, and **g+2**, which would explain the enhanced intensities of bands S, P, and N, respectively. However, small discrepancies between experimental IRMPD intensities and linear IR absorption cross sections may also arise from deficiencies of the computational approach and/or deviations of IRMPD signals from a linear behavior. Finally, the isomers with protonation at the indole N atom and the O atom of the hydroxyl group can be eliminated from the list of major carriers both from spectroscopic and energetic points of view, as their predicted IR spectra are clearly different from the measured IRMPD spectrum, and their relative energies are more than 100 kJ/mol above that of the **g-1** isomer.

The comparison between experimental and theoretical spectra (Table 1 and Figure 5) is clearly in favor of attributing the IRMPD spectrum largely to the **g-1** isomer. Several bands in the IRMPD spectrum correspond to single relatively intense calculated transitions of the **g-1** isomer (e.g., bands A–D, F–I, L–O, T, U, and W in Figures 4 and 5), whereas other bands are due to more than one significant vibrational mode. The maximum deviation of the positions of the experimental band maxima from the calculated frequencies is 29 cm<sup>-1</sup>, with an average deviation of 13 cm<sup>-1</sup>, confirming the vibrational and isomer assignments given in Table 1. In addition, all modes with calculated oscillator strengths larger than ~10 km/mol are visible in the experimental spectrum.

The weak bands A and B at 595 and 640 cm<sup>-1</sup> in the IRMPD spectrum of serotoninH<sup>+</sup> are assigned to aromatic  $\gamma_{\text{CC}}$  vibrations of the **g-1** isomer (see footnote d of Table 1 for the notation employed for vibrational modes). The weak feature C at 678 cm<sup>-1</sup> corresponds to a ring mode, whereas band D is again attributed to a low-intensity aromatic  $\gamma_{\text{CC}}$  mode. The high-intensity band E is composed of five closely overlapping aromatic  $\gamma_{\text{CH}}$  vibrations. The feature F at 840 cm<sup>-1</sup> is assigned to an isolated aliphatic symmetric  $\sigma_{\text{CCN}}$  mode. However, the stretching modes within the ethylamine side chain strongly couple with each other and with twisting, wagging and torsional

modes of the ethylamine side chain. Band G at  $936\text{ cm}^{-1}$  is attributed to a further isolated ring mode, whereas band H at  $961\text{ cm}^{-1}$  again is an aliphatic  $\sigma_{\text{CCN}}$  mode of the ethylamine side chain. The intensity of band H in the IRMPD spectrum appears somewhat enhanced compared to the calculated value. Band I at  $1027\text{ cm}^{-1}$  arises from an aliphatic CC stretch mode between C3 of the indole ring and C10 of the side chain. The feature K at  $1066\text{ cm}^{-1}$  is composed of the two close lying  $\text{CH}_2$  twisting vibrations located at C10 and C11 of the ethylamine side chain with nearly equal weight. Band L at  $1094\text{ cm}^{-1}$  is described as a coupled aromatic  $\beta_{\text{NH/CH}}$  mode of the indole ring. The intense band M is assigned to the isolated  $\delta_{\text{OH}}$  mode of the hydroxyl group. Band N at  $1220\text{ cm}^{-1}$  is dominated by the  $\tau_{\text{CH}_2}$  torsional mode located at C10 of the ethylamine side chain, with very weak contributions of an overlapping aromatic  $\beta_{\text{CH}}$  vibration. Band O at  $1263\text{ cm}^{-1}$  is assigned to a single aromatic  $\beta_{\text{CH}}$  mode. In contrast, band P at  $1304\text{ cm}^{-1}$  consists of two overlapping modes, the more intense being the  $\sigma_{\text{CO}}$  vibration and the less intense being the  $\tau_{\text{CH}_2}$  torsional mode at C11 of the ethylamine side chain. Four different vibrational modes produce band Q at  $1342\text{ cm}^{-1}$ . Two of them are the  $\beta_{\text{CH}_2}$  wagging modes at C10 and C11, and the third one is attributed to a further aromatic  $\beta_{\text{CH}}$  vibration. However, the by far strongest contribution comes from an aromatic CC stretch (corresponding to  $\nu_{14}$  in Wilson notation)<sup>33</sup> predicted at  $1371\text{ cm}^{-1}$  with high intensity. The somewhat larger red shift of about  $-30\text{ cm}^{-1}$  observed for this intense mode between the IRMPD and calculated frequency is ascribed to the IRMPD process, which shifts intense modes to lower frequency if other vibrations with significant intensity occur in the spectrum at slightly lower frequency.<sup>32</sup> The weak shoulder R at  $1417\text{ cm}^{-1}$  is probably the most prominent indicator for the assignment of **g-1** to the IRMPD spectrum. As mentioned above, this band should be the most intense feature in this spectral range, in the case of significant contributions from other gauche isomers (in disagreement with the experimental observation). On the basis of the **g-1** isomer, band R is assigned to two overlapping vibrations, namely a coupled  $\sigma_{\text{CC}}$  and  $\sigma_{\text{CN}}$  mode of the indole ring and the  $\beta_{\text{CH}_2}$  scissoring mode at C10 of the side chain. The broad band S at  $1454\text{ cm}^{-1}$  is a prominent feature in the IRMPD spectrum and also in the spectrum calculated for **g-1**. It consists of three almost equally intense fundamental transitions, namely, the in-phase and out-of-phase  $\beta_{\text{NH}_3}$  symmetric bending modes (umbrella mode) coupled with the  $\beta_{\text{CH}_2}$  scissoring mode at C11, and an aromatic  $\sigma_{\text{CC}}$  mode located at the phenol ring ( $\nu_{19a}$ ). The shoulder T at  $1499\text{ cm}^{-1}$  arises from a similar aromatic  $\sigma_{\text{CC}}$  mode ( $\nu_{19b}$ ) also located at the phenol ring. In contrast, band U at  $1542\text{ cm}^{-1}$  is due to an aromatic  $\sigma_{\text{CC}}$  mode of the pyrrole ring. The intense band V at  $1583\text{ cm}^{-1}$  is assigned to three overlapping transitions: the two asymmetric  $\beta_{\text{NH}_3}$  bending modes of the ammonium group and one aromatic  $\sigma_{\text{CC}}$  mode located at the phenol ring ( $\nu_{8b}$ ). The highest-frequency band in the measured spectral range is W at  $1624\text{ cm}^{-1}$  and is attributed to a further aromatic  $\sigma_{\text{CC}}$  mode of the phenol ring ( $\nu_{8a}$ ).

Comparison of the properties of neutral serotonin with those of serotoninH<sup>+</sup> establishes the effects of protonation on its geometric and electronic structure. The calculations predict an energetic preference for gauche isomers for both neutral and protonated serotonin, because they are stabilized through the intramolecular  $\text{NH}^{(+)}-\pi$  interaction with the aromatic indole ring. The major difference is that the neutral species prefers  $\text{NH}-\pi$  bonding to the pyrrole ring, whereas the protonated species interacts more effectively via  $\text{NH}^+-\pi$  bonding with the phenol ring (Figure F2 in the Supporting Information). In the

condensed phase, the preferential configuration of (protonated) serotonin changes drastically due to the effects of the environment. The interaction with solvent molecules and counterions is stronger than the intramolecular  $\text{NH}-\pi$  interaction and leads for both species to a preferential stabilization of trans conformers via intermolecular  $\text{NH}$  hydrogen bonding, although the gauche isomers are clearly calculated to be the global minima on the potential energy surface of the isolated species.

Interestingly, the present calculations at the B3LYP and MP2 level using the cc-pVDZ basis set yield a global minimum structure for neutral serotonin, denoted **g-2(n)**, which slightly differs from the global minimum derived previously at lower level calculations.<sup>10,12</sup> Calculations at the B3LYP/6-31G\* and MP2/6-31G\* yield a global minimum, denoted **Gpy(out)**, which is 0.7 or 2.5 kJ/mol more stable than the **Gpy(up)** conformation, which corresponds to **g-2(n)**. At the B3LYP/cc-pVDZ and MP2/cc-pVDZ level, the **g-2(n)** isomer is lower in energy than the **Gpy(out)** structure by 2.7 and 0.5 kJ/mol, respectively. These subtle differences illustrate the difficulties in predicting the energetic order of close lying isomers of these flexible molecules. Experimental evidence for the relative stability of the neutral serotonin isomers has been obtained from fluorescence and ionization yields,<sup>12</sup> which may, however, slightly depend on the conformation and ionization efficiency of the molecule and thus do not provide quantitative information about their stability.

In the following, we compare the properties of the most stable gauche structures of isolated serotonin(H<sup>+</sup>), **g-1** and **g+2(n)**, as obtained by the present quantum chemical calculations. Detailed structural parameters for both species are given in Figure F2 in the Supporting Information. The energy difference between both structures corresponds to the proton affinity of 967.6 (972.85) kJ/mol at the B3LYP (MP2) level. No experimental value appears to be available for comparison. As already mentioned, protonation drastically enhances the strength of the intramolecular  $\text{NH}-\pi$  interaction leading to substantially shorter contacts between the  $\text{NH}$  proton and the aromatic carbon atoms. Protonation at the N-terminus also leads to a small average elongation of the N-H bonds and simultaneously to an elongation of the neighboring N-C bond. All other bond length changes are less significant.

The structural changes induced by protonation of serotonin translate directly into the vibrational properties and the corresponding IR spectra, which are compared in Figure 5 in the fingerprint range. Clearly, protonation has a profound effect on both the positions and the IR intensities of the vibrational modes. The vibrational frequencies and IR intensities of **g+2(n)** and **g-1** obtained at the B3LYP level are compared in Table T3 in the Supporting Information, along with the assignment of the normal modes. As expected, the N-H bending modes experience the largest impact upon protonation in the frequency range investigated. All three N-H bend fundamentals have much larger IR intensities for the protonated species (band V) due to the large positive partial charge of the  $\text{NH}_3^+$  group. In particular, the intense symmetric N-H umbrella modes (here split into two modes due to coupling with  $\text{CH}_2$  scissoring modes) at  $1439$  and  $1445\text{ cm}^{-1}$  are characteristic for the charged **g-1** species (band S), whereas the IR spectrum of the neutral **g+2(n)** molecule has no intense absorption in this spectral range. On the other hand, the large intensity of the aromatic C-C stretch mode of **g+2(n)** at  $1499\text{ cm}^{-1}$  ( $\nu_{19b}$ , 103 km/mol) is largely reduced upon protonation ( $1508\text{ cm}^{-1}$ , 19 km/mol, band T). As there is no IR spectrum of isolated serotonin available in the literature in the fingerprint range, comparison of the IR spectrum

calculated for **g+2(n)** with experiment is not possible at the present stage.

The NBO population analysis for **g+2(n)** and **g-1**, is detailed in Figure F3 in the Supporting Information. As expected, the ethylamine side chain carries only little charge (0.03 e, B3LYP) in neutral serotonin and nearly the total positive charge (+0.97 e) in serotoninH<sup>+</sup>. The latter one is mainly localized on the ammonium group (+0.62 e) and to lesser extent in the adjacent CH<sub>2</sub> units (+0.30 and +0.05 e). The charge on the aromatic ring is not affected upon protonation, consistent with the lack of hyperconjugation in aromatic alkane derivatives. The large positive partial charge on the NH<sub>3</sub><sup>+</sup> group gives rise to the substantial charge-enhancement of the NH<sup>+</sup>- $\pi$  interaction in the **g-1** isomer of serotoninH<sup>+</sup> as compared to the neutral molecule.

Finally, the fragmentation process of serotoninH<sup>+</sup> is considered. The observed IRMPD fragment of serotoninH<sup>+</sup> is *m* = 160 u, corresponding to the loss of NH<sub>3</sub>. In contrast to dopamineH<sup>+</sup>,<sup>28</sup> for which fragmentation upon IRMPD occurs in a sequential fashion into various fragment channels, IRMPD of serotoninH<sup>+</sup> yields only one single fragment. Predominant loss of NH<sub>3</sub> upon collisional activation of serotoninH<sup>+</sup> has previously been observed by other groups.<sup>20</sup> Interestingly, Chang and Yeung report the elimination of the methylamine group (CH<sub>2</sub>NH<sub>2</sub>) to be the dominant fragmentation channel (*m* = 146 u).<sup>34</sup> However, it is likely that, due to their insufficient mass resolution, they were indeed observing the fragmentation of the serotonin<sup>+</sup> radical cation rather than serotoninH<sup>+</sup>, which was shown to eliminate CH<sub>2</sub>NH<sub>*n*</sub> with *n* = 1 and 2.<sup>35</sup> A variety of possible structures for the *m* = 160 u fragment ion observed upon IRMPD of **g-1** is shown in Figure F4 of the Supporting Information, along with their relative energies and dissociation energies for NH<sub>3</sub> elimination. However, it is difficult at the present stage to identify the actual structure of the fragment ion observed in the experiment.

#### 4. Concluding Remarks

The conformation and intramolecular cation- $\pi$  interactions of isolated serotoninH<sup>+</sup> were investigated by IRMPD spectroscopy and quantum chemical calculations. Comparison of the linear IR absorption spectra calculated for various gauche and trans conformers of serotoninH<sup>+</sup> and the experimental IRMPD spectrum in the fingerprint region yields the best agreement for the gauche conformer **g-1**, which is calculated to be the lowest-energy isomer at the B3LYP and MP2 level. In the **g-1** isomer, protonation occurs at the N-terminus of the ethylamine side chain, allowing for an efficient intramolecular NH<sup>+</sup>- $\pi$  cation- $\pi$  interaction of the ammonium group and the phenol moiety of the aromatic indole ring. Other isomers are higher in energy and have predicted IR spectra, which differ from the observed IRMPD spectrum, suggesting that **g-1** is the major carrier of the experimental spectrum. Although the cation- $\pi$  interaction in the gauche isomers of serotoninH<sup>+</sup> are largely governed by electrostatic and inductive contributions arising from the substantial positive charge localized mainly at the NH<sub>3</sub><sup>+</sup> group (~20–30 kJ/mol), dispersion contributions to the NH<sup>+</sup>- $\pi$  interaction (~7 kJ/mol) are inferred from the different stabilization energies obtained at the B3LYP and MP2 energies. Interestingly, this difference is only ~5 kJ/mol for dopamineH<sup>+</sup>, suggesting that the dispersion forces are larger in serotoninH<sup>+</sup> due to the interaction with the more extended aromatic  $\pi$ -electron system. The major differences between serotonin and its protonated form are that the excess charge strongly enhances the NH<sup>(+)</sup>- $\pi$  interaction and that protonation changes the

preferred binding motif from NH- $\pi$  bonding to the pyrrole ring to NH<sup>+</sup>- $\pi$  bonding to the phenol ring. Clearly, further experimental information about the strength of the NH<sup>+</sup>- $\pi$  interaction could come from IR spectra of serotoninH<sup>+</sup> recorded in the NH stretch range using optical parametric oscillator lasers.<sup>36</sup>

**Acknowledgment.** This work was supported by Technische Universität Berlin and Deutsche Forschungsgemeinschaft (DO 729/3). The research leading to these results has received funding from the European Community's Seventh Framework Programme (FP7/2007-2013) under Grant Agreement No. 226716. This work is part of the research program of FOM, which is financially supported by the Nederlandse Organisatie voor Wetenschappelijk Onderzoek (NWO). We gratefully acknowledge the excellent assistance by the FELIX staff (B. Redlich et al.).

**Supporting Information Available:** Geometries, energies, charge distributions, fragment ion structures, and vibrational properties of various serotoninH<sup>+</sup> isomers and neutral serotonin evaluated at various levels of theory. This material is available free of charge via the Internet at <http://pubs.acs.org>.

#### References and Notes

- (1) Mazak, K.; Doczy, V.; Kokosi, J.; Noszal, B. *Chem. Biodiversity* **2009**, 6 (4), 578. Frazer, A.; Hensler, J. G. In *Basic Neurochemistry: Molecular, Cellular and Medical Aspects*; Siegel, G. J., Agranoff, B. W., Albers, R. W., Fisher, S. K., Uhler, M. D., Eds.; Lippincott-Raven: Philadelphia, PA, 1999. (b) Hoyer, D.; Hannon, J. P.; Martin, G. R. *Pharmacol., Biochem. Behav.* **2002**, 71 (4), 533.
- (2) Declodet, E. H.; Stein, D. J. *Neuropsychiatr. Dis. Treat.* **2010**, 6, 233.
- (3) Soloff, P. H.; Price, J. C.; Meltzer, C. C.; Fabio, A.; Frank, G. K.; Kaye, W. H. *Biol. Psychiatry* **2007**, 62 (6), 580.
- (4) Paterson, D. S.; Trachtenberg, F. L.; Thompson, E. G.; Belliveau, R. A.; Beggs, A. H.; Darnall, R.; Chadwick, A. E.; Krous, H. F.; Kinney, H. C. *J. Am. Med. Assoc.* **2006**, 296 (17), 2124.
- (5) Pratuangdejkul, J.; Schneider, B.; Launay, J. M.; Kellermann, O.; Manivet, P. *Curr. Med. Chem.* **2008**, 15 (30), 3214.
- (6) Chattopadhyay, A.; Rukmini, R.; Mukherjee, S. *Biophys. J.* **1996**, 71 (4), 1952.
- (7) Beene, D. L.; Brandt, G. S.; Zhong, W. G.; Zacharias, N. M.; Lester, H. A.; Dougherty, D. A. *Biochemistry* **2002**, 41 (32), 10262.
- (8) Pisterzi, L. F.; Almeida, D. R. P.; Chass, G. A.; Torday, L. L.; Papp, J. G.; Varro, A.; Cszizmadia, I. G. *Chem. Phys. Lett.* **2002**, 365 (5–6), 542.
- (9) Mazurek, A. P.; Weinstein, H.; Osman, R.; Topiol, S.; Ebersole, B. J. *Int. J. Quantum Chem.* **1984**, 183.
- (10) van Mourik, T.; Emson, L. E. V. *Phys. Chem. Chem. Phys.* **2002**, 4 (23), 5863.
- (11) Bayari, S.; Saglam, S.; Ustundag, H. F. *J. Mol. Struct.-THEOCHEM* **2005**, 726 (1–3), 225.
- (12) LeGreve, T. A.; Baquero, E. E.; Zwier, T. S. *J. Am. Chem. Soc.* **2007**, 129 (13), 4028.
- (13) Alagona, G.; Ghio, C.; Nagy, P. I. *J. Chem. Theory Comput.* **2005**, 1 (5), 801.
- (14) Pratuangdejkul, J.; Jaudon, P.; Ducrocq, C.; Nosoongnoen, W.; Guerin, G. A.; Conti, M.; Loric, S.; Launay, J. M.; Manivet, P. *J. Chem. Theory Comput.* **2006**, 2 (3), 746.
- (15) Alagona, G.; Ghio, C. *J. Mol. Struct.-THEOCHEM* **2006**, 769 (1–3), 123.
- (16) LeGreve, T. A.; Clarkson, J. R.; Zwier, T. S. *J. Phys. Chem. A* **2008**, 112 (17), 3911. LeGreve, T. A.; James, W. H.; Zwier, T. S. *J. Phys. Chem. A* **2009**, 113 (2), 399.
- (17) Ison, R. R.; Roberts, G. C. K.; Partington, P. J. *Pharm. Pharmacol.* **1972**, 24 (1), 82.
- (18) Bugg, C. E.; Thewalt, U. *Science* **1970**, 170 (3960), 852. Amit, A.; Mester, L.; Klewe, B.; Furberg, S. *Acta Chem. Scand., Ser. A: Phys. Inorg. Chem.* **1978**, 32 (3), 267. Karle, L.; Dragonet, Ks.; Brenner, S. A. *Acta Crystallogr.* **1965**, 19, 713.
- (19) Thewalt, U.; Bugg, C. E. *Acta Crystallogr., Sect. B: Struct. Crystallogr. Cryst. Chem.* **1972**, 28, 82.
- (20) Thomson, B. A.; Iribarne, J. V.; Dziedzic, P. *J. Anal. Chem.* **1982**, 54 (13), 2219. Steiner, W. E.; Clowers, B. H.; English, W. A.; Hill, H. H.

*Rapid Commun. Mass Spectrom.* **2004**, *18* (8), 882. Bourcier, S.; Hoppilliard, Y. *Rapid Commun. Mass Spectrom.* **2009**, *23* (1), 93.

(21) Bourcier, S.; Benoist, J. F.; Clerc, F.; Rigal, O.; Taghi, M.; Hoppilliard, Y. *Rapid Commun. Mass Spectrom.* **2006**, *20* (9), 1405.

(22) Macleod, N. A.; Simons, J. P. *Mol. Phys.* **2006**, *104* (20–21), 3317. Macleod, N. A.; Simons, J. P. *Phys. Chem. Chem. Phys.* **2004**, *6*, 2821. Vaden, T. D.; de Boer, T.; MacLeod, N. A.; Marzluff, E. M.; Simons, J. P.; Snoek, L. C. *Phys. Chem. Chem. Phys.* **2007**, *9* (20), 2549.

(23) Eyler, J. R. *Mass Spectrom. Rev.* **2009**, *28* (3), 448. Polfer, N. C.; Oomens, J. *Mass Spectrom. Rev.* **2009**, *28* (3), 468. Knorke, H.; Langer, J.; Oomens, J.; Dopfer, O. *Astrophys. J. Lett.* **2009**, 706. L66. Seydou, M.; Gregoire, G.; Liquier, J.; Lemaire, J.; Schermann, J. P.; Desfrancois, C. *J. Am. Chem. Soc.* **2008**, *130* (12), 4187. Fridgen, T. D. *Mass Spectrom. Rev.* **2009**, *28* (4), 586.

(24) Zhao, D. W.; Langer, J.; Oomens, J.; Dopfer, O. *J. Chem. Phys.* **2009**, *131*, 131.

(25) Rizzo, T. R.; Stearns, J. A.; Boyarkin, O. V. *Int. Rev. Phys. Chem.* **2009**, *28* (3), 481. Nagornova, N. S.; Rizzo, T. R.; Boyarkin, O. V. *J. Am. Chem. Soc.* **2010**, *132* (12), 4040. Fujihara, A.; Matsumoto, H.; Shibata, Y.; Ishikawa, H.; Fuke, K. *J. Phys. Chem. A* **2008**, *112* (7), 1457. Guidi, M.; Lorenz, U. J.; Papadopoulos, G.; Boyarkin, O. V.; Rizzo, T. R. *J. Phys. Chem. A* **2009**, *113* (5), 797. Stearns, J. A.; Guidi, M.; Boyarkin, O. V.; Rizzo, T. R. *J. Chem. Phys.* **2007**, *127* (15), 154322.

(26) MacAleese, L.; Maitre, P. *Mass Spectrom. Rev.* **2007**, *26* (4), 583. Dopfer, O. *J. Phys. Org. Chem.* **2006**, *19*, 540. Lagutschenkov, A.; Springer, A.; Lorenz, U. J.; Maitre, P.; Dopfer, O. *J. Phys. Chem. A* **2010**, *114* (5), 2073. Lagutschenkov, A.; Sinha, R. K.; Maitre, P.; Dopfer, O. *J. Phys. Chem. A* **2010**, *114* (42), 11053.

(27) O. Dopfer, Report for Project FELIX-003 (2009).

(28) Lagutschenkov, A.; Langer, J.; Berden, G.; Oomens, J.; Dopfer, O. *Phys. Chem. Chem. Phys.*, in press.

(29) Valle, J. J.; Eyler, J. R.; Oomens, J.; Moore, D. T.; van der Meer, A. F. G.; von Helden, G.; Meijer, G.; Hendrickson, C. L.; Marshall, A. G.;

Blakney, G. T. *Rev. Sci. Instrum.* **2005**, *76* (2), 7. Oepts, D.; Vandermeer, A. F. G.; Vanamersfoort, P. W. *Infrared Phys. Technol.* **1995**, *36* (1), 297.

(30) Dunning, T. H. *J. Chem. Phys.* **1989**, *90* (2), 1007.

(31) Frisch, M. J.; Trucks, G. W.; Schlegel, H. B.; Scuseria, G. E.; Robb, M. A.; Cheeseman, J. R.; Montgomery, J. A., Jr.; Vreven, T.; Kudin, K. N.; Burant, J. C.; Millam, J. M.; Iyengar, S. S.; Tomasi, J.; Barone, V.; Mennucci, B.; Cossi, M.; Scalmani, G.; Rega, N.; Petersson, G. A.; Nakatsuji, H.; Hada, M.; Ehara, M.; Toyota, K.; Fukuda, R.; Hasegawa, J.; Ishida, M.; Nakajima, T.; Honda, Y.; Kitao, O.; Nakai, H.; Klene, M.; Li, X.; Knox, J. E.; Hratchian, H. P.; Cross, J. B.; Bakken, V.; Adamo, C.; Jaramillo, J.; Gomperts, R.; Stratmann, R. E.; Yazyev, O.; Austin, A. J.; Cammi, R.; Pomelli, C.; Ochterski, J. W.; Ayala, P. Y.; Morokuma, K.; Voth, G. A.; Salvador, P.; Dannenberg, J. J.; Zakrzewski, V. G.; Dapprich, S.; Daniels, A. D.; Strain, M. C.; Farkas, O.; Malick, D. K.; Rabuck, A. D.; Raghavachari, K.; Foresman, J. B.; Ortiz, J. V.; Cui, Q.; Baboul, A. G.; Clifford, S.; Cioslowski, J.; Stefanov, B. B.; Liu, G.; Liashenko, A.; Piskorz, P.; Komaromi, I.; Martin, R. L.; Fox, D. J.; Keith, T.; Al-Laham, M. A.; Peng, C. Y.; Nanayakkara, A.; Challacombe, M.; Gill, P. M. W.; Johnson, B.; Chen, W.; Wong, M. W.; Gonzalez, C.; Pople, J. A. *Gaussian 03*, revision C.02; Gaussian, Inc.: Wallingford, CT, 2004.

(32) Oomens, J.; Sartakov, B. G.; Meijer, G.; Von Helden, G. *Int. J. Mass Spectrom.* **2006**, *254* (1–2), 1.

(33) Wilson, E. B. *Phys. Rev.* **1934**, *45* (10), 706.

(34) Chang, S. Y.; Yeung, E. S. *Anal. Chem.* **1997**, *69* (13), 2251.

(35) Cardoso, A. M.; Correla, A. J. F. *Eur. J. Mass Spectrom.* **1999**, *5* (1), 11.

(36) Pasker, F.; Solca, N.; Dopfer, O. *J. Phys. Chem. A* **2006**, *110*, 12793. Andrei, H.-S.; Solca, N.; Dopfer, O. *ChemPhysChem* **2006**, *7*, 107. Andrei, H.-S.; Solca, N.; Dopfer, O. *J. Phys. Chem. A* **2005**, *109*, 3598. Dopfer, O. *Z. Phys. Chem.* **2005**, *219*, 125. Solca, N.; Dopfer, O. *Phys. Chem. Chem. Phys.* **2004**, *6*, 2732. Solca, N.; Dopfer, O. *Eur. Phys. J. D* **2002**, *20*, 469. Bieske, E. J.; Dopfer, O. *Chem. Rev.* **2000**, *100*, 3963.

JP109337A